Appl. Phys. B 78, 171–177 (2004)
DOI: 10.1007/s00340-003-1365-6

Applied Physics B
Lasers and Optics

P. MAHNKE✉
H.H. KLINGENBERG

Observation and analysis of mode competition in optic parametric oscillators

Institut für Technische Physik, Deutsches Zentrum für Luft- und Raumfahrt (DLR), Pfaffenwaldring 38–40, 70569 Stuttgart, Germany

Received: 7 February 2003/Revised version: 14 October 2003
Published online: 19 December 2003 • © Springer-Verlag 2003

ABSTRACT We report on an experimental investigation and an analytical description of mode competition in an optical parametric ring oscillator (OPO). A ring cavity was spectrally controlled by injection seeding techniques. Upon injecting the signal wavelength at a power level of 2 mW the relevant idler wave was generated and monitored through a 2 cm long methane absorption cell. Mode competition was observable when two seedlasers operating at almost the same signal wavelengths were injected collinearly into the OPO. Both seedlasers were about 0.5 nm apart, and within the same acceptance bandwidth of the used nonlinear crystal (KTP). Simultaneous injection of the two seedlasers was performed by keeping the resonator dependent gain of one injected wavelength parameterized while the other was tuned. The influence of one seedlaser on the second was measured by using the generated idler waves, and the absorption cell as a monitor. We observed three types of operation mutually dependent on the seedlaser wavelengths: a free running OPO, one seedlaser seeding the OPO, and both seedlasers seeding the OPO at the same time.

PACS 42.65.Yj; 42.79.Nv; 42.79.Qx

1 Introduction

Optical parametric oscillators (OPOs) have been demonstrated and used in the past for their great potential as continuously tunable radiation sources [1–3]. When pumped with an intense pulse of a solid-state laser, for example with a nanosecond long Nd:YAG laser pulse, OPOs can be build as a compact and rugged all-solid-state device with a broadband tuning capability from the ultraviolet to the near infrared [4, 5]. Together with high output pulse energies and conversion efficiencies OPOs became attractive for many applications in research and industry, like laser induced fluorescence spectroscopy [6], pump-probe experiments using either the same [7, 8], or two different wavelengths [9], one for exciting the species and the other for probing a relaxed state. Such a radiation source is also of interest as a transmitter for monitoring environmental trace gases. Many applications also require, besides the suitable wavelength, a bandwidth of the OPO which is considerably smaller than the spectral width of a molecular species to be investigated. To control the spectral properties of an OPO it is convenient to use wavelength selective elements, like filters or etalons for narrowing its spectral width [10]. Employing additional optical elements within the cavity is disadvantageous because further losses are produced which reduce the overall efficiency. Another well established means for reducing the bandwidth of an OPO is controlling the spectral properties by the technique of injection seeding, first reported by Bjorkholm and Danielmeyer [11], for further information see [12]. The smallest spectral widths of OPOs can be obtained by using continuous-wave seed sources, as have been demonstrated by using dye lasers [13], Ti:sappire lasers [14] or color-center lasers [15]. For our planned remote sensing application we chose commercially available external cavity diode lasers (New Focus, Vortex 6031) based on the Littman Metcalf design [16, 17] utilizing a blazed diffraction grating at grazing incidence for wavelength selection.

We developed a pump laser/OPO system for monitoring methane. The built transmitting and receiving system needed to be robust and compact. Since such systems are mostly installed on a mobile or an aerial platform the previously mentioned all-solid-state devices are preferred. For applying the differential absorption lidar (DIAL) technique for the investigation of a particular absorbing species, one needs to transmit two adjacent wavelengths λ–on and λ–off, respectively [17–20]. The wavelength λ–on is absorbed by the trace gas and λ–off, which is not absorbed, is used as a reference. To provide the relevant DIAL wavelength for methane detection, an injection-seeded Nd:YAG laser is used to pump an OPO generating the IR wavelength, around 3.3 μm. Stable operation can be achieved at these two wavelengths by using two different external cavity diode lasers as injection seed sources. For practical reasons we chose to operate the OPO signal as resonant. About 2 mW seed power at the signal wavelength was sufficient to obtain the preferred idler waves (λ–on and λ–off).

The two seedlasers were superimposed and injected into the resonator at the same time. Therefore, alternatively one or the other seedlaser seeded the OPO. Wavelength selection between the seed-wavelengths can be realized by shifting the whole gain profile of the OPO crystal synchronously with the pulse repetition rate. This method can be realized by tilting the OPO crystal and is used if the wavelength difference of both

✉ Fax: +49-711/6862-715, E-mail: peter.mahnke@dlr.de

seedlasers is larger than the OPO acceptance bandwidth [17]. For our application a wavelength difference within the acceptance bandwidth of the nonlinear crystal was chosen such that both seedlasers could eventually seed the OPO at the same time.

In the experimental part we report on the investigation of mode competition between the two wavelengths when both seedlasers are operated near a mode of the resonator. This is performed by studying the dependence of the injection seeding process through modulation of the frequency of one seedlaser while the other was kept at a constant frequency offset to its adjacent resonator mode. We repeated this measurement for several fixed frequency offsets. We chose to increase the offset from the center of the mode. This is to our knowledge the first reported mode competition experiment on a dual signal wave injection seeded OPO.

Finally, in the last part of this report we describe the observations following the well known mode competition analysis [21].

2 Experimental setup and results

Figure 1 shows the experimental setup. A travelling wave ring KTP-OPO is injection seeded by two electrically tunable external cavity diode lasers operating around 1580 nm (Seedlaser 1, 2). The bandwidth of each seedlaser is smaller than 300 kHz. Both seedlasers were coupled with a fifty percent mirror and injected into the OPO cavity. The power injected by each seedlaser was approximately 1 mW. Seeding with similar conditions was also demonstrated before by Milton et al. [22]. For a rugged design the OPO cavity was machined from a solid aluminum block to ensure thermal and vibrational stability. A resonator stability of better than 100 MHz/min was observed. The OPO was pumped with a diode pumped injection seeded Q-switched Nd-YAG laser with a pulse length of 13 ns, a repetition rate of 100 Hz, 3 Watt average power and a spot size of 1.1 mm. The nonlinear medium was a 16 mm long KTP crystal with antireflection coating for the pump, signal and idler radiation. The crystal was cut for type II (o $\rightarrow$ oe) phase matching ($\theta = 82°$, $\phi = 0°$). This results in a theoretical acceptance bandwidth of 5.8 $cm^{-1} \approx 174$ GHz [23]. The free spectral range of the OPO ring resonator was 3.7 GHz. The ring resonator was designed to be signal resonant and consisted of three plane mirrors. The input coupler was coated for high transmission of the pump, and reflection of the signal wavelength. The output coupler had a high transmission coating for both the pump and idler wavelength, and 5% transmission for the signal wavelength. The turning mirror was a highly reflective mirror for the mid infrared region. In unseeded operation the threshold of the OPO was at 7.9 mJ and in seeded operation the threshold of the OPO was at 6.2 mJ of pump energy. When pumped with 15 mJ we achieved in seeded operation a signal energy of 2 mJ and an idler energy of 1 mJ of the OPO.

Successful seeding of the signal wave narrows the broad free running OPO spectrum to the two injected wavelengths (and their corresponding idler wavelengths), which can be detected by measuring the OPO power. The pulse build up time of the OPO is reduced in the seeded regime significantly [24], thus the overall power of an injection seeded pulse is higher than the power of a free running system. The signal and idler bandwidths of a single mode seeded OPO is lower than 100 MHz. This limit is given by the measured pulse duration of the OPO (10 ns, with a nearly gaussian pulse shape).

For analyzing the injection seeding process of the signal wave the corresponding idler wave was sent through a 2 cm long absorption cell containing 800 mbar of methane. The signal and seedlaser wavelengths were blocked by a germanium long pass filter (LP). The right hand side of Fig. 1 characterizes the absorption cell for different seedlaser frequency offsets of one seedlaser indicated by the idler intensity before and behind the absorption cell. The free running OPO spectrum is partly absorbed by the cell and is used as a reference intensity, which is set to one, in the figure. When the seedlaser was tuned to a longitudinal mode of the OPO resonator an increase of power was observed, i.e. the OPO is seeded. For this case, spectral narrowing is revealed by a different absorption compared with the one from the free running

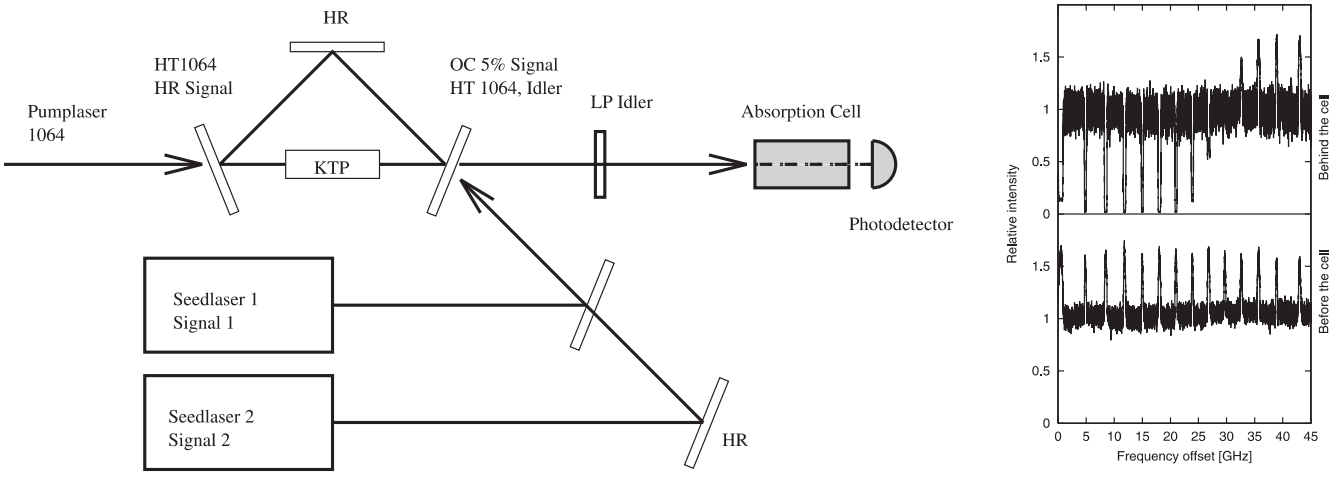

FIGURE 1 Experimental setup of the double injection seeded OPO. The inset on the right shows the operational characteristics of the absorption cell used as a diagnostic instrument for the injection seeding process. The top curve displays the photo detector signal behind the cell versus the frequency detuning. The bottom curve shows the measured idler intensity with a second detector placed in front of the cell. When seeded, an increase of intensity is observed. This is the case when the seedlaser frequency hits the longitudinal mode comb of the OPO resonator

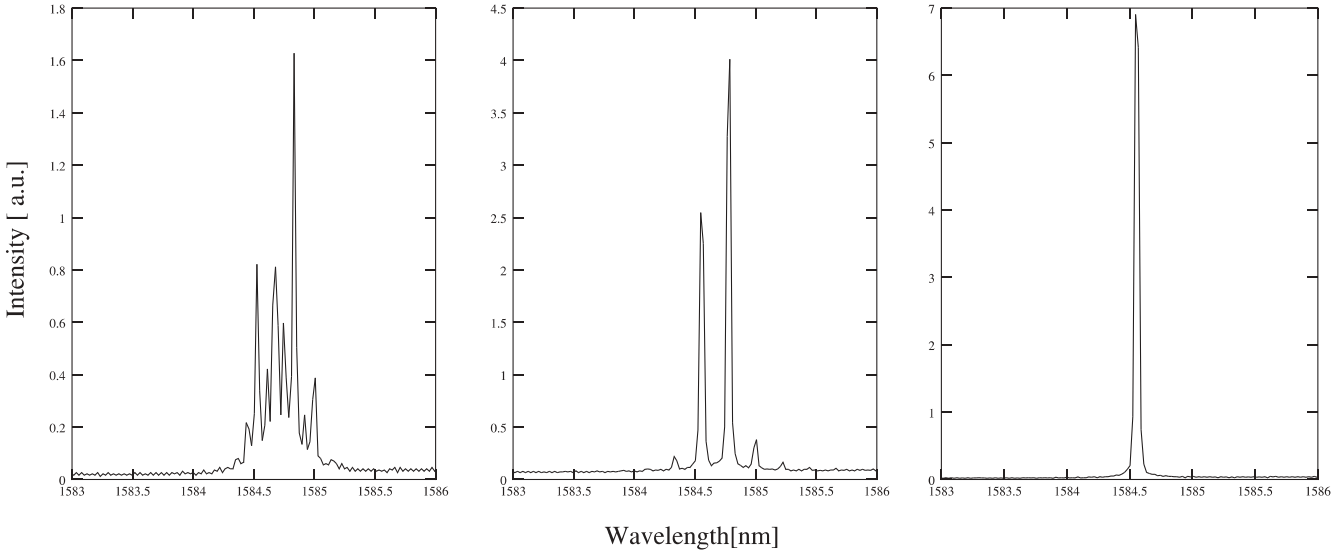

FIGURE 2 Signal wave spectra: (From left to right) 1. Spectrum of the free running OPO, 2. Spectrum of the OPO seeded by both seedlasers simultaneously, 3. Single mode spectrum of the OPO

spectrum. For continuous spectroscopy of methane in this wavelength region see ref. [25]. To distinguish between the two seed wavelengths according to our application, seedlaser (1) was tuned to a mode where the corresponding idler wavelength was totally absorbed from the methane cell (λ–on). Therefore, successful seeding of the λ–on mode could be detected by a maximum absorption in the gas cell. The second seedlaser (2), called λ–off, was tuned to a mode with a corresponding non absorbed idler wave. Injection seeding the λ–off mode results in an increased detector signal behind the cell. Both seeded wavelengths were about seven ($\Delta\omega = 25$ GHz) to ten ($\Delta\omega = 37$ GHz) longitudinal modes apart.

In Fig. 2 three signal wave spectra of the OPO are depicted. The spectra were measured with a high resolution (approximately 50 pm) spectrometer MSD1000 from SOLAR TII with a Hamamatsu InGaAs diode array as detector. The left spectrum is the spectrum of the free running OPO. A spectral width of 0.4 nm, approximately 50 GHz, was observed. Both wavelengths of the seedlasers are in the acceptance bandwidth of the OPO. In the second picture, dual mode operation of the OPO is shown. This spectrum can be observed when both seedlasers seed the system simultaneously. The observed sidebands result from difference- and sum-frequency mixing with the difference-frequency or sum-frequency of the two injected modes. The separation of the side modes from the injected modes is an integer multiple of the difference frequency of the seeded modes. In the measured case the two seedlasers are about eight longitudinal resonator modes apart. About five percent of the measured signal intensity was spread into the sidebands. Possible ways of generation could be the following:

– Optical rectification of signal and idler radiation:

$$\omega_{s_{\lambda_{on}}} - \omega_{s_{\lambda_{off}}} \rightarrow \Delta\omega$$
$$\omega_{i_{\lambda_{off}}} - \omega_{i_{\lambda_{on}}} \rightarrow \Delta\omega\,,$$

with the seeded frequencies given by the λ–on and λ–off signal- and idler-frequencies $\omega_{s,i_{\lambda_{on,off}}}$, respectively. A sum frequency back mixing process results in the observed side bands.

– Sum-frequency generation of non corresponding (λ–on, λ–off) signal and idler waves results in a broadening of the pump radiation:

$$\omega_{s_{\lambda_{on}}} + \omega_{i_{\lambda_{off}}} \rightarrow \omega_{pump+\Delta\omega}$$
$$\omega_{s_{\lambda_{off}}} + \omega_{i_{\lambda_{on}}} \rightarrow \omega_{pump-\Delta\omega}$$

A difference frequency back mixing process of $\omega_{pump-\Delta\omega}$ and $\omega_{pump+\Delta\omega}$ with signal and idler radiation results in the observed side bands.

Both lie within the acceptance bandwidth of the phase matching and can be studied utilizing spectroscopy of the depleted pump light as well as in the radio frequency region, but is not investigated in this work. The third spectrum shows single mode operation of the system. This occurs when only one seedlaser seeds the system. In the following we describe how these different states of the system are obtained.

Next in Fig. 3 the measured transmitted intensity through the absorption cell for detuning the two seed lasers operated independently is shown. Only one laser at a time was used for seeding during this measurement. We detuned the seedlasers electrically over a total range of 1.2 GHz around the center of the injection seeding range. On-line seeded operation, which corresponds to spectrum 3 in Fig. 2, can be clearly seen through total absorption of the idler wave, detected with a photodiode. The off-line seeded operation results in a higher intensity level. The free running transmitted intensity, which corresponds to spectrum 1, was set arbitrarily to one. The observed injection seeding ranges for the absorbed longitudinal and non absorbed longitudinal mode were about 500 MHz, which is in the order of magnitude of the spectral width of the low finesse resonator. For the non absorbed mode a dependence of the power and the seedlaser frequency offset from the center of the adjacent mode was observed – which corresponds to the wavelength amplification by the resonator.

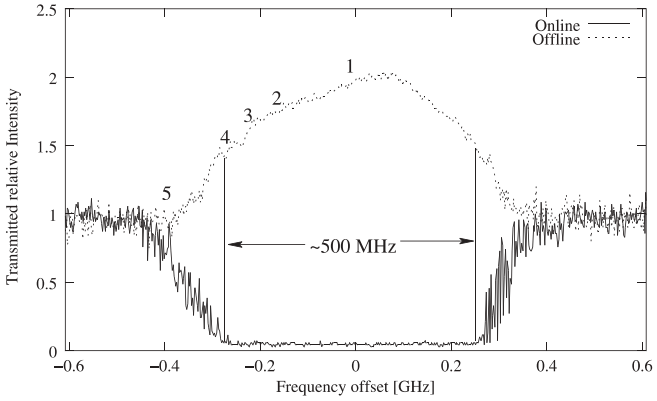

FIGURE 3 Intensity measured behind the absorption cell for independent detuning of the two seedlasers. The injection seeding range of the off-line and on-line wavelength can be seen clearly because of the higher photodiode signal for the off-line seeded case and the lower photodiode signal for the on-line seeded case. The numbers, 1 to 5, indicate different detunings of the off-line seedlaser from the center of the injection seeding range, corresponding to the measurements presented in Fig. 4

The numbers in the figure indicate different detunings of the non absorbed seedlaser for the next measurement, where both seedlasers were injected into the resonator at the same time.

The measurements presented in Fig. 4 illustrate the reduction of the λ–on seedlasers injection seeding range, through the existence of a second injection seeder operating at a constant wavelength difference to a second resonator mode (λ–off). The reduction of the seeding range can be explained with mode competition effects between the two seeded modes. The set of curves was realized by scanning the wavelength of the λ–on seedlaser while keeping the λ–off seedlaser on constant offsets which are indicated in Fig. 3. For the measurements the λ–off seedlaser was tuned from the center of the non absorbed injection seeded longitudinal cavity mode to the edge of the injection seeding range. The top curve (no. 1) resulted from the smallest detuning of the λ–off seedlaser from the center of the injection seeding range, and the bottom curve (no. 5) resulted from a detuning larger than 300 MHz which is just outside the injection seeding range. The injection seeding

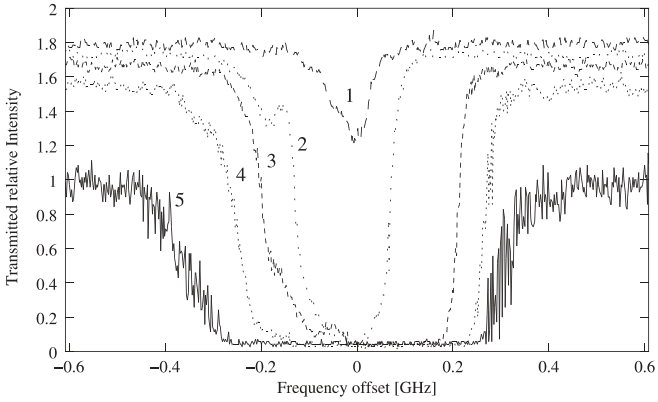

FIGURE 4 Intensity of the non absorbed (λ–off) injection seeded wavelength versus detuning of the absorbed (λ–on) injection seeder from the center of the injection seeding range. The intensity of the unseeded OPO is set to 1. The different curves are for various detunings from the λ–off seeder from the center of its injection seeding range. Higher Intensities have a smaller detuning from the center of the λ–off seeding range

Curve	Offline detuning [GHz]	Online seeding range [GHz]	Range of coexistence [GHz]
5	0.5±0.05	0.51±0.05	0.83±0.05
4	0.24	0.42	0.72
3	0.22	0.26	0.55
2	0.18	0.03	0.43
1	0.15	0	0.24

TABLE 1 Measured injection seeding ranges for different frequency offsets (see Fig. 4). The online seeding range is the region where only the λ–on signal and idler radiation is emitted. The range of coexistence is the range where λ–on and λ–off or only λ–on is seeded

range of the absorbed longitudinal cavity mode (λ–on) grows for larger detunings of the λ–off seedlaser. Between the regions where only one wavelength seeds the OPO, regions with both wavelength can be observed (spectrum 2 of Fig. 2). In the case of the top curve (no. 1) there is no region where only the λ–on seedlaser seeds the system, resulting in partial absorption of the corresponding idler waves, since only the λ–on idler wave is absorbed by the cell. During the measurements no thermal drift of the resonator length occurred. This can be easily verified since the intensity of the λ–off seeded wavelength is the same for large positive and negative detunings of the λ–on seedlaser. Table 1 lists the measured injection seeding ranges and the range of coexistence for the different curves shown in Fig. 4. The measured λ–on injection seeding range is the range of λ–on detuning where only λ–on seeds the system. The coexistence range is the range in which the influence of the λ–on seedlaser on the λ–off seeding can be observed.

3 Two-mode competition analysis

To analyze and describe the competition between two injection seeded longitudinal modes in an optical parametric oscillator, we followed the approximation of a coupled saturated oscillator as described by Siegman [21]. In the case of an injection seeded pump laser the gain mechanism of the OPO behaves like a homogeneously broadened gain process because the whole signal and idler spectrum is generated by one pump wavelength only. The coupling mechanisms in the nanosecond injection seeded regime is given by the coupled wave equations [26]. In the following, parameters for λ–on will be indicated by the index 1 and parameters for λ–off will be indicated by the index 2:

$$\frac{\partial E_p}{\partial z} = 2\mathrm{i}\frac{\omega_\mathrm{p}^2 d_\mathrm{eff}}{k_\mathrm{p} c^2} E_{\mathrm{s}_1} E_{\mathrm{i}_1} \mathrm{e}^{-\mathrm{i}\Delta k_1} + 2\mathrm{i}\frac{\omega_p^2 d_\mathrm{eff}}{k_\mathrm{p} c^2} E_{\mathrm{s}_2} E_{\mathrm{i}_2} \mathrm{e}^{-\mathrm{i}\Delta k_1}$$

$$\frac{\partial E_{\mathrm{s}_{1,2}}}{\partial z} = 2\mathrm{i}\frac{\omega_\mathrm{p}^2 d_\mathrm{eff}}{k_{\mathrm{s}_{1,2}} c^2} E_\mathrm{p} E^*_{\mathrm{i}_{1,2}} \mathrm{e}^{\mathrm{i}\Delta k_{1,2}}$$

$$\frac{\partial E_{\mathrm{i}_{1,2}}}{\partial z} = 2\mathrm{i}\frac{\omega_\mathrm{p}^2 d_\mathrm{eff}}{k_{\mathrm{i}_{1,2}} c^2} E_\mathrm{p} E^*_{\mathrm{s}_{1,2}} \mathrm{e}^{\mathrm{i}\Delta k_{1,2}}$$

with

$$\Delta k_{1,2} = k_\mathrm{p} - k_{\mathrm{s}_{1,2}} - k_{\mathrm{i}_{1,2}} ,$$

and the following notations: $E_{\mathrm{p,s,i}}$ is the field strength of the pump-, signal- and idler-waves, the parametric coefficient is d_eff, and $k_{\mathrm{p,s,i}}$ are the corresponding wavenumbers.

The small-signal parametric gain for a single pass through the crystal can be calculated by considering a constant pump power over the length of the crystal. With this assumption we get for $\Delta k = 0$ from the coupled wave equations for the second derivatives of the fields:

$$\frac{\partial^2 E_{\mathrm{s,i}_{1,2}}}{\partial z^2} = \frac{4\omega_\mathrm{p}^4 d_\mathrm{eff}^2 E_\mathrm{p}^2}{k_{\mathrm{i}_{1,2}} k_{\mathrm{s}_{1,2}} c^2} E_{\omega_{\mathrm{s,i}_{1,2}}}$$

By solving this differential equation a small-signal gain for the electric field for a certain crystal length can be deduced. For a small-signal gain of the signal and idler intensities we get:

$$G = \frac{4\omega_\mathrm{p}^4 d_\mathrm{eff}^2 E_\mathrm{p}^2}{k_{\mathrm{i}_{1,2}} k_{\mathrm{s}_{1,2}} c^2} L_\mathrm{Crystal}^2$$

It should be noted that for higher signal and idler powers the gain process must be modelled differently, since a constant pump power over the whole crystal length cannot be assumed. Processes, like pump depletion can be expected, and will take a significant part of the pump power away and saturate the gain. When the pump power is higher than twice the threshold power of the OPO, additional back mixing effects may have to be considered for the parametric process too.

In the low power limit a first order approximation of the gain process can be described by the self- and cross saturation coefficients for modelling the nonlinear gain process. This approach will be valid as long as there is no other significant back conversion process occurring. A significant back conversion process would broaden the pump pulse and result in an inhomogeneously broadened gain process. In the singely built resonant OPO this assumption holds, because the idler and the broadened pump radiation leaves the resonator after a single pass through the crystal. That is why we can model the two longitudinal mode OPO as a self- and cross-saturated coupled oscillator.

The coupled intensity equations of a self saturating coupled oscillator can be written as follows [21]:

$$\frac{\mathrm{d}}{\mathrm{d}t}\begin{pmatrix} I_{\mathrm{s}_1} \\ I_{\mathrm{s}_2} \end{pmatrix} = \begin{pmatrix} \left(\alpha_1(\Delta\omega_1) - \beta_1 I_{\mathrm{s}_1} - \phi_{12} I_{\mathrm{s}_2}\right) I_{\mathrm{s}_1} \\ \left(\alpha_2(\Delta\omega_2) - \beta_2 I_{\mathrm{s}_2} - \phi_{21} I_{\mathrm{s}_1}\right) I_{\mathrm{s}_2} \end{pmatrix} \quad (1)$$

The coefficients $\alpha_i(\Delta\omega_i)$ are the small-signal or unsaturated gains minus the seed-wavelength dependent losses of each mode. The coefficients β_i and ϕ_{ij} represent the first order self- and cross-saturation coefficients of the optical parametric system, which are expected to be of the same order of magnitude, because the loss mechanisms through pump depletion are the same . If we assume for simplicity, a square pump pulse, the coefficients can be taken as constants. In ref. [24] it is shown that in such a system the intensities start growing exponentially before saturation effects take over. The saturation lasts as long as the pump pulse is applied. From the steady-state analysis of the system we learn about the dynamic systems behavior since the dynamic solution of the system is attracted by the steady-state solution. The dynamic stability of the steady-state solutions can be determined by a perturbation stability analysis which shows when the solution is attracting or repulsing. The $\Delta\omega_i$ dependency of α_i results from the wavelength-offset dependent gain of the injection seeded longitudinal oscillator mode. The wavelength dependency of the gain can be described by a combination of the resonator Airy function and the acceptance function of the parametric process which is given by $(\sin(\frac{\Delta kl}{2})/\frac{\Delta kl}{2})^2$.

3.1 *Steady-state solutions*

The differential equations ((1)) have three possible steady-state solutions ($\frac{\mathrm{d}I}{\mathrm{d}t} = 0$):

1. $I_{\mathrm{s}_{1,\mathrm{ss}}} = 0$ and $I_{\mathrm{s}_{2,\mathrm{ss}}} = \dfrac{\alpha_2(\Delta\omega_2)}{\beta_2}$
2. $I_{\mathrm{s}_{2,\mathrm{ss}}} = 0$ and $I_{\mathrm{s}_{1,\mathrm{ss}}} = \dfrac{\alpha_1(\Delta\omega_1)}{\beta_1}$
3. $I_{\mathrm{s}_{1,\mathrm{ss}}} = \dfrac{\alpha_1(\Delta\omega_1)\beta_2 - \alpha_2(\Delta\omega_2)\phi_{12}}{\beta_1\beta_2 - \phi_{12}\phi_{21}}$ and
   $I_{\mathrm{s}_{2,\mathrm{ss}}} = \dfrac{\alpha_2(\Delta\omega_2)\beta_1 - \alpha_1(\Delta\omega_1)\phi_{21}}{\beta_1\beta_2 - \phi_{12}\phi_{21}}$.

The third solution is only a reasonable solution for positive intensities I. If we assume that the self saturation coefficients β_i are larger than the cross saturation coefficients ϕ_{ij} we get only positive solutions if $\frac{\alpha_2\beta_1}{\phi_{21}} > \alpha_1 > \frac{\alpha_2\phi_{12}}{\beta_2}$.

3.2 *Perturbation stability analysis*

To analyze the stability of these solutions, we linearize the differential equations ((1)) around the steady-state solutions. The perturbed intensities $I_{\mathrm{s}_1}(t)$ and $I_{\mathrm{s}_2}(t)$ are written as follows: $I_{\mathrm{s}_1}(t) = I_{\mathrm{s}_{1,\mathrm{ss}}} + \epsilon_1(t)$ and $I_{\mathrm{s}_2}(t) = I_{\mathrm{s}_{2,\mathrm{ss}}} + \epsilon_2(t)$. With this approximation the differential equation reads:

$$\frac{\mathrm{d}}{\mathrm{d}t}\begin{pmatrix} \varepsilon_1 \\ \varepsilon_2 \end{pmatrix} = \begin{pmatrix} \alpha_1 - 2\beta_1 I_{\mathrm{s}_{1,\mathrm{ss}}} - \phi_{12} I_{\mathrm{s}_{2,\mathrm{ss}}} & -\phi_{12} I_{\mathrm{s}_{1,\mathrm{ss}}} \\ -\phi_{21} I_{\mathrm{s}_{2,\mathrm{ss}}} & \alpha_2 - 2\beta_2 I_{\mathrm{s}_{2,\mathrm{ss}}} - \phi_{21} I_{\mathrm{s}_{1,\mathrm{ss}}} \end{pmatrix} \begin{pmatrix} \varepsilon_1 \\ \varepsilon_2 \end{pmatrix}$$

The stability of this linear differential equation is determined by the eigenvalues of the perturbation matrix. For negative eigenvalues the differential equation is stable. The eigenvalue problem must be solved for all steady-state solutions. The resulting different stability regions for the three steady-state solutions are:

1. $\begin{pmatrix} \alpha_1 - \dfrac{\phi_{12}\alpha_2}{\beta_2} & 0 \\ -\dfrac{\phi_{21}\alpha_2}{\beta_2} & -\alpha_2 \end{pmatrix}$ which is stable if $\alpha_1 < \dfrac{\phi_{12}\alpha_2}{\beta_2}$.
2. $\begin{pmatrix} -\alpha_1 & -\dfrac{\phi_{12}\alpha_1}{\beta_1} \\ 0 & \alpha_2 - \dfrac{\phi_{21}\alpha_1}{\beta_1} \end{pmatrix}$ which is stable if $\alpha_1 > \dfrac{\alpha_2\beta_1}{\phi_{21}}$.
3. $\begin{pmatrix} -\beta_1 I_{\mathrm{s}_{1,\mathrm{ss}}} & -\phi_{12} I_{\mathrm{s}_{2,\mathrm{ss}}} \\ -\phi_{21} I_{\mathrm{s}_{2,\mathrm{ss}}} & -\beta_2 I_{\mathrm{s}_{2,\mathrm{ss}}} \end{pmatrix}$ with $I_{\mathrm{s}_{1,\mathrm{ss}}} = \dfrac{\alpha_1\beta_2 - \alpha_2\phi_{12}}{\beta_1\beta_2 - \phi_{12}\phi_{21}}$ and
   $I_{\mathrm{s}_{2,\mathrm{ss}}} = \dfrac{\alpha_2\beta_1 - \alpha_1\phi_{21}}{\beta_1\beta_2 - \phi_{12}\phi_{21}}$.

This results in the following non overlapping stability regions:

1. For $\alpha_1 < \dfrac{\phi_{12}\alpha_2}{\beta_2}$ the intensities $I_{s_{1,2}}$ are attracted by $I_{\mathrm{s}_{1,\mathrm{ss}}} = 0$ and $I_{\mathrm{s}_{2,\mathrm{ss}}} = \dfrac{\alpha_2(\Delta\omega_2)}{\beta_2}$

2. For $\alpha_1 > \dfrac{\alpha_2\beta_1}{\phi_{21}}$ the intensities are attracted by $I_{s_{2,ss}} = 0$ and
$$I_{s_{1,ss}} = \frac{\alpha_1(\Delta\omega_1)}{\beta_1}$$
3. For $\dfrac{\alpha_2\beta_1}{\phi_{21}} > \alpha_1 > \dfrac{\alpha_2\phi_{12}}{\beta_2}$ the intensities are attracted by
$$I_{s_{1,ss}} = \frac{\alpha_1\beta_2 - \alpha_2\phi_{12}}{\beta_1\beta_2 - \phi_{12}\phi_{21}} \text{ and}$$
$$I_{s_{2,ss}} = \frac{\alpha_2\beta_1 - \alpha_1\phi_{21}}{\beta_1\beta_2 - \phi_{12}\phi_{21}}.$$

With the assumption of a square pump pulse and a short pulse build up in the resonator we can conclude that the overall intensities of the pulsed injection seeded system will be attracted to the steady-state solutions.

Figure 5 illustrates the dependency of the three stability regions from the gain-loss coefficient α_1. The coefficient α_1 complies with the λ–on wavelength dependent gain. The curves show the α_1 dependency of the steady state intensities for the two different wavelengths. For $\alpha_1 < \frac{\phi_{12}\alpha_2}{\beta_2}$ we are in region 1 were the intensity $I_{s_{2,ss}}$ wins the mode competition. There is no α_1 dependency of the intensities in this regions. For values of α_1 in the interval $\frac{\alpha_2\beta_1}{\phi_{21}} > \alpha_1 > \frac{\alpha_2\phi_{12}}{\beta_2}$ (region 3) there is a coexistence of both waves and $I_{s_{1,ss}}$ grows in proportion to the gain α_1 whereas $I_{s_{2,ss}}$ decreases with an increase in the gain of $I_{s_{1,ss}}$. When α_1 is larger than $\frac{\alpha_2\beta_1}{\phi_{21}}$ the intensity $I_{s_{1,ss}}$ wins the mode competition (region 2). Again a proportional growth of the intensity with its gain parameter can be observed. The cross-saturation coupling parameters $\phi_{12,21}$ are chosen as smaller than the self-saturation parameters $\beta_{1,2}$ because we observed in the experiment (Fig. 4) regions where both lasers seeded the OPO resonator modes, which corresponds to region 3.

A further result of the analysis is that the intensity is directly proportional to the gain-loss coefficient α if only one laser seeds the system. This enables us to take the measured λ–off seeded curve from Fig. 3 as proportional to $\alpha(\Delta\omega)$. This measured gain-loss coefficient will be similar for other injection seeded longitudinal resonator modes since the wavelength dependency of the gain-loss coefficient resulting from the nonlinear process (acceptance function of the parametric process) will only scale the magnitude of this wavelength dependency. So we can choose a wavelength dependent gain for α_1 like the one measured from our resonator (Fig. 3).

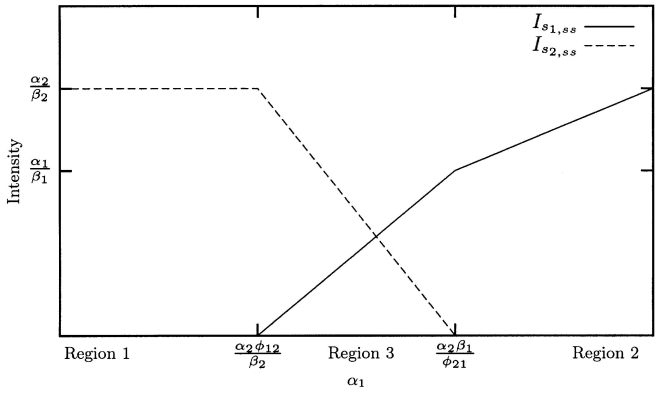

FIGURE 5 Dependence of the intensities on the gain parameter α_1. The three different stability regions are indicated

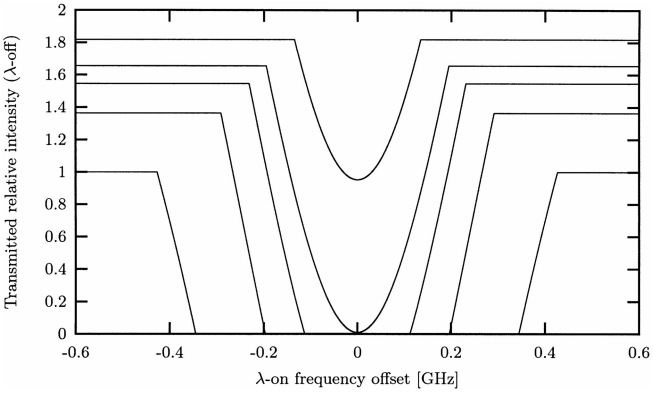

FIGURE 6 Simulation of the non absorbed injection seeded wavelength for different constant gain-loss coefficients α_2 and a wavelength dependent gain-loss coefficient $\alpha_1(\Delta\omega)$. The coefficient $\alpha_1(\Delta\omega)$ follows the curve form measured in Fig. 3

To simulate our experimental results, shown in Fig. 4, we need to choose a wavelength dependent gain for the small-signal gain-loss coefficient α_1 as described above. This is performed by fitting a second order polynomial to the measured seeding frequency dependence on the intensity shown in Fig. 3. Furthermore, we need to choose the α_2 dependent width of region 3 with the two parameters $\frac{\phi_{12}}{\beta_2}$ and $\frac{\beta_1}{\phi_{21}}$, which can also be done to fit the measured data. The simulation of the experiment is performed utilizing various constant gain-loss coefficients α_2 while scanning the frequency-offset $\Delta\omega_1$, which changes the gain-loss parameter $\alpha_1(\Delta\omega_1)$. The result, I_2 versus $\Delta\omega_1$, is depicted in Fig. 6 which is in qualitative agreement to the measured values. The narrowing of the λ–on injection seeding range results from the constant maximum value of α_1, while higher values of α_2 shift the minimum limit of stability of region 2 (where only λ–on is seeded) to higher values. Even the complete distinction of region 2 can be observed, when the maximum value of α_1 cannot reach the upper limit of region 3. The upper limit of region 1 is shifted for higher values of α_2 too.

4 Conclusions and outlook

We demonstrated and analytically described mode competition in a dual injection seeded OPO. The applied model delivered a qualitative description of the measured mode competition effects and the narrowing of the injection seeding ranges. It was shown that the injection seeding range is dependent on the gain of other injected (and free running) modes. It should be noted, although not demonstrated here, that for wavelength switching applications the wavelength dependent gain of a resonator can be used to separate injection seeding ranges. This could be realized by shifting the longitudinal mode structure of the resonator with a piezo element, which changes the resonator length from pulse to pulse. Correctly synchronized with the pump lasers repetition rate, the OPO resonator gets the same mode comb for every second pump pulse. Adjusting each seedlaser on one mode comb enables fast switching between two wavelengths without mode competition effects.

Furthermore, we observed inter mode mixing effects in a parametric oscillator and found out that the efficiency of this process is high enough to be taken into account for exact spectral simulations of parametric processes. These could be investigated by high resolution spectroscopy of the depleted pump and in the region of the wavelength difference.

ACKNOWLEDGEMENTS We gratefully acknowledge R. Bähnisch and G. Spindler for helpful discussions. Thanks go to C. Lemmerz for the help with the measurements, and to A. Hoffstädt from Adlares GmbH for use of their nice spectrometer. This work was financially supported by the Ruhrgas AG.

REFERENCES

1 R.L. Byer: In: *Quantum Electronics: A Treatise*, Vol. 1, Part A, H. Rabin, C.L. Tang (Academic Press, NY 1975) pp. 587–702
2 C.L. Tang, W.R. Bosenberg, T. Ukachi, R.J. Lane, L.K. Cheng: Proc. IEEE **80**, 365 (1992)
3 F.J. Duarte (Ed.): *Tunable Laser Applications* (Marcel Dekker, Inc., NY 1995)
4 Y.X. Fan, R.C. Eckardt, R.L. Byer, J. Nolting, R. Wallenstein: Appl. Phys. Lett. **53**, 2014 (1988)
5 L.K. Cheng, W.R. Bosenberg, C.L. Tang: Appl. Phys. Lett. **53**, 175 (1988)
6 R. Giezendanner, O. Keck, P. Weigand, W. Meier, U. Meier, W. Stricker, A. Aigner: Combust. Sci. Technol. **175**, 721 (2003)
7 D. von der Linde, J. Kuhl, H.H. Klingenberg: Phys. Rev. Lett. **44**, 1505 (1980)
8 A. Laubereau, in: *Ultrashort Laser Pulses*, W. Kaiser (Springer-Verlag, Berlin, Heidelberg, NY 1993) pp. 35–112
9 M. Volk, G. Aumeier, T. Häberle, A. Ogrodnik, R. Feick, M.E. Michel-Beyerle: Biochim. Biophys. Acta **1102**, 253 (1992)
10 W.R. Bosenberg, W.S. Pelouch, C.L. Tang: Appl. Phys. Lett. **55**, 1952 (1989)
11 J.E. Bjorkholm, H.G. Danielmeyer: Appl. Phys. Lett. **15**, 171 (1969)
12 W. Koechner: *Solid-State Laser Engeneering* (Springer, Heidelberg 1999)
13 O. Votava, J.R. Flair, D.F. Plusquellic, E. Riedle, D.J. Nesbitt: J. Chem. Phys. **107**, 8854 (1997)
14 T.D. Raymond, W.J. Alford, A.V. Smith, M.S. Bowers: Opt. Lett. **19**, 1520 (1994)
15 D.C. Hovde, J.H. Timmermans, G. Scoles, K.K. Lehmann: Opt. Commun. **86**, 294 (1991)
16 M.G. Littman, H.J. Metcalf: Opt. Lett. **3**, 138 (1978)
17 M.J.T. Milton, T.D. Gardiner, F. Molero, J. Galech: Opt. Commun. **142**, 153 (1997)
18 R.M. Schotland: Proc. 4th Symp. Remote Sensing of the Environment, Uni. of Michigan Press, Ann Arbor (1966) p. 273
19 R.M. Schotland: J. Appl. Meteor. **13**, 71 (1974)
20 R.M. Measures: *Laser Remote Sensing* (Wiley, NY 1984)
21 A.E. Siegman: *Lasers* (Uni. Sci. Books, 1986) pp. 992–1003
22 M.J.T. Milton, T.D. Gardiner, G. Chourdakis, P.T. Woods: Opt. Lett. **19**, 281 (1994)
23 A.V. Smith: *SNLO nonlinear optics code*. Sandia Nat. Lab., Albuquerque, NM 87185-1423.
24 A.E. Siegman: Appl. Opt. **1**, 739 (1962)
25 G.W. Baxter, H.D. Barth, B.J. Orr: Appl. Phys. B **66**, 653 (1998)
26 R.L. Sutherland: *Handbook of Nonlinear Optics* (Marcel Dekker, Inc., NY 1996)